# Measurement of Inclusive Jet Cross Sections in $Z/\gamma^*(\to e^+e^-) +$ jets Production in $p\bar{p}$ Collisions at $\sqrt{s} = 1.96$ TeV

T. Aaltonen,[23] J. Adelman,[13] T. Akimoto,[54] M. G. Albrow,[17] B. Álvarez González,[11] S. Amerio,[42] D. Amidei,[34] A. Anastassov,[51] A. Annovi,[19] J. Antos,[14] M. Aoki,[24] G. Apollinari,[17] A. Apresyan,[47] T. Arisawa,[56] A. Artikov,[15] W. Ashmanskas,[17] A. Attal,[3] A. Aurisano,[52] F. Azfar,[41] P. Azzi-Bacchetta,[42] P. Azzurri,[45] N. Bacchetta,[42] W. Badgett,[17] A. Barbaro-Galtieri,[28] V. E. Barnes,[47] B. A. Barnett,[25] S. Baroiant,[7] V. Bartsch,[30] G. Bauer,[32] P.-H. Beauchemin,[33] F. Bedeschi,[45] P. Bednar,[14] S. Behari,[25] G. Bellettini,[45] J. Bellinger,[58] A. Belloni,[22] D. Benjamin,[16] A. Beretvas,[17] J. Beringer,[28] T. Berry,[29] A. Bhatti,[49] M. Binkley,[17] D. Bisello,[42] I. Bizjak,[30] R. E. Blair,[2] C. Blocker,[6] B. Blumenfeld,[25] A. Bocci,[16] A. Bodek,[48] V. Boisvert,[48] G. Bolla,[47] A. Bolshov,[32] D. Bortoletto,[47] J. Boudreau,[46] A. Boveia,[10] B. Brau,[10] A. Bridgeman,[24] L. Brigliadori,[5] C. Bromberg,[35] E. Brubaker,[13] J. Budagov,[15] H. S. Budd,[48] S. Budd,[24] K. Burkett,[17] G. Busetto,[42] P. Bussey,[21] A. Buzatu,[33] K. L. Byrum,[2] S. Cabrera,[16,a] M. Campanelli,[35] M. Campbell,[34] F. Canelli,[17] A. Canepa,[44] D. Carlsmith,[58] R. Carosi,[45] S. Carrillo,[18,b] S. Carron,[33] B. Casal,[11] M. Casarsa,[17] A. Castro,[5] P. Catastini,[45] D. Cauz,[53] M. Cavalli-Sforza,[3] A. Cerri,[28] L. Cerrito,[30,c] S. H. Chang,[27] Y. C. Chen,[1] M. Chertok,[7] G. Chiarelli,[45] G. Chlachidze,[17] F. Chlebana,[17] K. Cho,[27] D. Chokheli,[15] J. P. Chou,[22] G. Choudalakis,[32] S. H. Chuang,[51] K. Chung,[12] W. H. Chung,[58] Y. S. Chung,[48] C. I. Ciobanu,[24] M. A. Ciocci,[45] A. Clark,[20] D. Clark,[6] G. Compostella,[42] M. E. Convery,[17] J. Conway,[7] B. Cooper,[30] K. Copic,[34] M. Cordelli,[19] G. Cortiana,[42] F. Crescioli,[45] C. Cuenca Almenar,[7,a] J. Cuevas,[11,d] R. Culbertson,[17] J. C. Cully,[34] D. Dagenhart,[17] M. Datta,[17] T. Davies,[21] P. de Barbaro,[48] S. De Cecco,[50] A. Deisher,[28] G. De Lentdecker,[48,e] G. De Lorenzo,[3] M. Dell'Orso,[45] L. Demortier,[49] J. Deng,[16] M. Deninno,[5] D. De Pedis,[50] P. F. Derwent,[17] G. P. Di Giovanni,[43] C. Dionisi,[50] B. Di Ruzza,[53] J. R. Dittmann,[4] M. D'Onofrio,[3] S. Donati,[45] P. Dong,[8] J. Donini,[42] T. Dorigo,[42] S. Dube,[51] J. Efron,[38] R. Erbacher,[7] D. Errede,[24] S. Errede,[24] R. Eusebi,[17] H. C. Fang,[28] S. Farrington,[29] W. T. Fedorko,[13] R. G. Feild,[59] M. Feindt,[26] J. P. Fernandez,[31] C. Ferrazza,[45] R. Field,[18] G. Flanagan,[47] R. Forrest,[7] S. Forrester,[7] M. Franklin,[22] J. C. Freeman,[28] I. Furic,[18] M. Gallinaro,[49] J. Galyardt,[12] F. Garberson,[10] J. E. Garcia,[45] A. F. Garfinkel,[47] H. Gerberich,[24] D. Gerdes,[34] S. Giagu,[50] V. Giakoumopolou,[45,f] P. Giannetti,[45] K. Gibson,[46] J. L. Gimmell,[48] C. M. Ginsburg,[17] N. Giokaris,[15,f] M. Giordani,[53] P. Giromini,[19] M. Giunta,[45] V. Glagolev,[15] D. Glenzinski,[17] M. Gold,[36] N. Goldschmidt,[18] A. Golossanov,[17] G. Gomez,[11] G. Gomez-Ceballos,[32] M. Goncharov,[52] O. González,[31] I. Gorelov,[36] A. T. Goshaw,[16] K. Goulianos,[49] A. Gresele,[42] S. Grinstein,[22] C. Grosso-Pilcher,[13] R. C. Group,[17] U. Grundler,[24] J. Guimaraes da Costa,[22] Z. Gunay-Unalan,[35] C. Haber,[28] K. Hahn,[32] S. R. Hahn,[17] E. Halkiadakis,[51] A. Hamilton,[20] B.-Y. Han,[48] J. Y. Han,[48] R. Handler,[58] F. Happacher,[19] K. Hara,[54] D. Hare,[51] M. Hare,[55] S. Harper,[41] R. F. Harr,[57] R. M. Harris,[17] M. Hartz,[46] K. Hatakeyama,[49] J. Hauser,[8] C. Hays,[41] M. Heck,[26] A. Heijboer,[44] B. Heinemann,[28] J. Heinrich,[44] C. Henderson,[32] M. Herndon,[58] J. Heuser,[26] S. Hewamanage,[4] D. Hidas,[16] C. S. Hill,[10,g] D. Hirschbuehl,[26] A. Hocker,[17] S. Hou,[1] M. Houlden,[29] S.-C. Hsu,[9] B. T. Huffman,[41] R. E. Hughes,[38] U. Husemann,[59] J. Huston,[35] J. Incandela,[10] G. Introzzi,[45] M. Iori,[50] A. Ivanov,[7] B. Iyutin,[32] E. James,[17] B. Jayatilaka,[16] D. Jeans,[50] E. J. Jeon,[27] S. Jindariani,[18] W. Johnson,[7] M. Jones,[47] K. K. Joo,[27] S. Y. Jun,[12] J. E. Jung,[27] T. R. Junk,[24] T. Kamon,[52] D. Kar,[18] P. E. Karchin,[57] Y. Kato,[40] R. Kephart,[17] U. Kerzel,[26] V. Khotilovich,[52] B. Kilminster,[38] D. H. Kim,[27] H. S. Kim,[27] J. E. Kim,[27] M. J. Kim,[17] S. B. Kim,[27] S. H. Kim,[54] Y. K. Kim,[13] N. Kimura,[54] L. Kirsch,[6] S. Klimenko,[18] M. Klute,[32] B. Knuteson,[32] B. R. Ko,[16] S. A. Koay,[10] K. Kondo,[56] D. J. Kong,[27] J. Konigsberg,[18] A. Korytov,[18] A. V. Kotwal,[16] J. Kraus,[24] M. Kreps,[26] J. Kroll,[44] N. Krumnack,[4] M. Kruse,[16] V. Krutelyov,[10] T. Kubo,[54] S. E. Kuhlmann,[2] T. Kuhr,[26] N. P. Kulkarni,[57] Y. Kusakabe,[56] S. Kwang,[13] A. T. Laasanen,[47] S. Lai,[33] S. Lami,[45] S. Lammel,[17] M. Lancaster,[30] R. L. Lander,[7] K. Lannon,[38] A. Lath,[51] G. Latino,[45] I. Lazzizzera,[42] T. LeCompte,[2] J. Lee,[48] J. Lee,[27] Y. J. Lee,[27] S. W. Lee,[52,h] R. Lefèvre,[20] N. Leonardo,[32] S. Leone,[45] S. Levy,[13] J. D. Lewis,[17] C. Lin,[59] C. S. Lin,[28] J. Linacre,[41] M. Lindgren,[17] E. Lipeles,[9] A. Lister,[7] D. O. Litvintsev,[17] T. Liu,[17] N. S. Lockyer,[44] A. Loginov,[59] M. Loreti,[42] L. Lovas,[14] R.-S. Lu,[1] D. Lucchesi,[42] J. Lueck,[26] C. Luci,[50] P. Lujan,[28] P. Lukens,[17] G. Lungu,[18] L. Lyons,[41] J. Lys,[28] R. Lysak,[14] E. Lytken,[47] P. Mack,[26] D. MacQueen,[33] R. Madrak,[17] K. Maeshima,[17] K. Makhoul,[32] T. Maki,[23] P. Maksimovic,[25] S. Malde,[41] S. Malik,[30] G. Manca,[29] A. Manousakis,[15,f] F. Margaroli,[47] C. Marino,[26] C. P. Marino,[24] A. Martin,[59] M. Martin,[25] V. Martin,[21,i] M. Martínez,[3] R. Martínez-Ballarín,[31] T. Maruyama,[54] P. Mastrandrea,[50] T. Masubuchi,[54] M. E. Mattson,[57] P. Mazzanti,[5] K. S. McFarland,[48] P. McIntyre,[52] R. McNulty,[29,j] A. Mehta,[29] P. Mehtala,[23] S. Menzemer,[11,k] A. Menzione,[45] P. Merkel,[47] C. Mesropian,[49] A. Messina,[35] T. Miao,[17] N. Miladinovic,[6] J. Miles,[32] R. Miller,[35] C. Mills,[22] M. Milnik,[26] A. Mitra,[1] G. Mitselmakher,[18] H. Miyake,[54] S. Moed,[22] N. Moggi,[5] C. S. Moon,[27] R. Moore,[17] M. Morello,[45] P. Movilla Fernandez,[28] J. Mülmenstädt,[28] A. Mukherjee,[17] Th. Muller,[26]

 

R. Mumford,[25] P. Murat,[17] M. Mussini,[5] J. Nachtman,[17] Y. Nagai,[54] A. Nagano,[54] J. Naganoma,[56] K. Nakamura,[54] I. Nakano,[39] A. Napier,[55] V. Necula,[16] C. Neu,[44] M. S. Neubauer,[24] J. Nielsen,[28,l] L. Nodulman,[2] M. Norman,[9] O. Norniella,[24] E. Nurse,[30] S. H. Oh,[16] Y. D. Oh,[27] I. Oksuzian,[18] T. Okusawa,[40] R. Oldeman,[29] R. Orava,[23] K. Osterberg,[23] S. Pagan Griso,[42] C. Pagliarone,[45] E. Palencia,[17] V. Papadimitriou,[17] A. Papaikonomou,[26] A. A. Paramonov,[13] B. Parks,[38] S. Pashapour,[33] J. Patrick,[17] G. Pauletta,[53] M. Paulini,[12] C. Paus,[32] D. E. Pellett,[7] A. Penzo,[53] T. J. Phillips,[16] G. Piacentino,[45] J. Piedra,[43] L. Pinera,[18] K. Pitts,[24] C. Plager,[8] L. Pondrom,[58] X. Portell,[3] O. Poukhov,[15] N. Pounder,[41] F. Prakoshyn,[15] A. Pronko,[17] J. Proudfoot,[2] F. Ptohos,[17,m] G. Punzi,[45] J. Pursley,[58] J. Rademacker,[41,g] A. Rahaman,[46] V. Ramakrishnan,[58] N. Ranjan,[47] I. Redondo,[31] B. Reisert,[17] V. Rekovic,[36] P. Renton,[41] M. Rescigno,[50] S. Richter,[26] F. Rimondi,[5] L. Ristori,[45] A. Robson,[21] T. Rodrigo,[11] E. Rogers,[24] S. Rolli,[55] R. Roser,[17] M. Rossi,[53] R. Rossin,[10] P. Roy,[33] A. Ruiz,[11] J. Russ,[12] V. Rusu,[17] H. Saarikko,[23] A. Safonov,[52] W. K. Sakumoto,[48] G. Salamanna,[50] O. Saltó,[3] L. Santi,[53] S. Sarkar,[50] L. Sartori,[45] K. Sato,[17] A. Savoy-Navarro,[43] T. Scheidle,[26] P. Schlabach,[17] E. E. Schmidt,[17] M. A. Schmidt,[13] M. P. Schmidt,[59] M. Schmitt,[37] T. Schwarz,[7] L. Scodellaro,[11] A. L. Scott,[10] A. Scribano,[45] F. Scuri,[45] A. Sedov,[47] S. Seidel,[36] Y. Seiya,[40] A. Semenov,[15] L. Sexton-Kennedy,[17] A. Sfyria,[20] S. Z. Shalhout,[57] M. D. Shapiro,[28] T. Shears,[29] P. F. Shepard,[46] D. Sherman,[22] M. Shimojima,[54,n] M. Shochet,[13] Y. Shon,[58] I. Shreyber,[20] A. Sidoti,[45] P. Sinervo,[33] A. Sisakyan,[15] A. J. Slaughter,[17] J. Slaunwhite,[38] K. Sliwa,[55] J. R. Smith,[7] F. D. Snider,[17] R. Snihur,[33] M. Soderberg,[34] A. Soha,[7] S. Somalwar,[51] V. Sorin,[35] J. Spalding,[17] F. Spinella,[45] T. Spreitzer,[33] P. Squillacioti,[45] M. Stanitzki,[59] R. St. Denis,[21] B. Stelzer,[8] O. Stelzer-Chilton,[41] D. Stentz,[37] J. Strologas,[36] D. Stuart,[10] J. S. Suh,[27] A. Sukhanov,[18] H. Sun,[55] I. Suslov,[15] T. Suzuki,[54] A. Taffard,[24,o] R. Takashima,[39] Y. Takeuchi,[54] R. Tanaka,[39] M. Tecchio,[34] P. K. Teng,[1] K. Terashi,[49] J. Thom,[17,p] A. S. Thompson,[21] G. A. Thompson,[24] E. Thomson,[44] P. Tipton,[59] V. Tiwari,[12] S. Tkaczyk,[17] D. Toback,[52] S. Tokar,[14] K. Tollefson,[35] T. Tomura,[54] D. Tonelli,[17] S. Torre,[19] D. Torretta,[17] S. Tourneur,[43] W. Trischuk,[33] Y. Tu,[44] N. Turini,[45] F. Ukegawa,[54] S. Uozumi,[54] S. Vallecorsa,[20] N. van Remortel,[23] A. Varganov,[34] E. Vataga,[36] F. Vázquez,[18,b] G. Velev,[17] C. Vellidis,[45,f] V. Veszpremi,[47] M. Vidal,[31] R. Vidal,[17] I. Vila,[11] R. Vilar,[11] T. Vine,[30] M. Vogel,[36] I. Volobouev,[28,h] G. Volpi,[45] F. Würthwein,[9] P. Wagner,[44] R. G. Wagner,[2] R. L. Wagner,[17] J. Wagner-Kuhr,[26] W. Wagner,[26] T. Wakisaka,[40] R. Wallny,[8] S. M. Wang,[1] A. Warburton,[33] D. Waters,[30] M. Weinberger,[52] W. C. Wester III,[17] B. Whitehouse,[55] D. Whiteson,[44,o] A. B. Wicklund,[2] E. Wicklund,[17] G. Williams,[33] H. H. Williams,[44] P. Wilson,[17] B. L. Winer,[38] P. Wittich,[17,p] S. Wolbers,[17] C. Wolfe,[13] T. Wright,[34] X. Wu,[20] S. M. Wynne,[29] A. Yagil,[9] K. Yamamoto,[40] J. Yamaoka,[51] T. Yamashita,[39] C. Yang,[59] U. K. Yang,[13,q] Y. C. Yang,[27] W. M. Yao,[28] G. P. Yeh,[17] J. Yoh,[17] K. Yorita,[13] T. Yoshida,[40] G. B. Yu,[48] I. Yu,[27] S. S. Yu,[17] J. C. Yun,[17] L. Zanello,[50] A. Zanetti,[53] I. Zaw,[22] X. Zhang,[24] Y. Zheng,[8,r] and S. Zucchelli[5]

(CDF Collaboration)

[1]*Institute of Physics, Academia Sinica, Taipei, Taiwan 11529, Republic of China*
[2]*Argonne National Laboratory, Argonne, Illinois 60439, USA*
[3]*Institut de Fisica d'Altes Energies, Universitat Autonoma de Barcelona, E-08193, Bellaterra (Barcelona), Spain*
[4]*Baylor University, Waco, Texas 76798, USA*
[5]*Istituto Nazionale di Fisica Nucleare, University of Bologna, I-40127 Bologna, Italy*
[6]*Brandeis University, Waltham, Massachusetts 02254, USA*
[7]*University of California, Davis, Davis, California 95616, USA*
[8]*University of California, Los Angeles, Los Angeles, California 90024, USA*
[9]*University of California, San Diego, La Jolla, California 92093, USA*
[10]*University of California, Santa Barbara, Santa Barbara, California 93106, USA*
[11]*Instituto de Fisica de Cantabria, CSIC-University of Cantabria, 39005 Santander, Spain*
[12]*Carnegie Mellon University, Pittsburgh, Pennsylvania 15213, USA*
[13]*Enrico Fermi Institute, University of Chicago, Chicago, Illinois 60637, USA*
[14]*Comenius University, 842 48 Bratislava, Slovakia; Institute of Experimental Physics, 040 01 Kosice, Slovakia*
[15]*Joint Institute for Nuclear Research, RU-141980 Dubna, Russia*
[16]*Duke University, Durham, North Carolina 27708*
[17]*Fermi National Accelerator Laboratory, Batavia, Illinois 60510, USA*
[18]*University of Florida, Gainesville, Florida 32611, USA*
[19]*Laboratori Nazionali di Frascati, Istituto Nazionale di Fisica Nucleare, I-00044 Frascati, Italy*
[20]*University of Geneva, CH-1211 Geneva 4, Switzerland*
[21]*Glasgow University, Glasgow G12 8QQ, United Kingdom*
[22]*Harvard University, Cambridge, Massachusetts 02138, USA*

[23]Division of High Energy Physics, Department of Physics, University of Helsinki and Helsinki Institute of Physics, FIN-00014, Helsinki, Finland
[24]University of Illinois, Urbana, Illinois 61801, USA
[25]The Johns Hopkins University, Baltimore, Maryland 21218, USA
[26]Institut für Experimentelle Kernphysik, Universität Karlsruhe, 76128 Karlsruhe, Germany
[27]Center for High Energy Physics: Kyungpook National University, Daegu 702-701, Korea; Seoul National University, Seoul 151-742, Korea; Sungkyunkwan University, Suwon 440-746, Korea; Korea Institute of Science and Technology Information, Daejeon, 305-806, Korea; Chonnam National University, Gwangju, 500-757, Korea
[28]Ernest Orlando Lawrence Berkeley National Laboratory, Berkeley, California 94720, USA
[29]University of Liverpool, Liverpool L69 7ZE, United Kingdom
[30]University College London, London WC1E 6BT, United Kingdom
[31]Centro de Investigaciones Energeticas Medioambientales y Tecnologicas, E-28040 Madrid, Spain
[32]Massachusetts Institute of Technology, Cambridge, Massachusetts 02139, USA
[33]Institute of Particle Physics: McGill University, Montréal, Canada H3A 2T8; and University of Toronto, Toronto, Canada M5S 1A7
[34]University of Michigan, Ann Arbor, Michigan 48109, USA
[35]Michigan State University, East Lansing, Michigan 48824, USA
[36]University of New Mexico, Albuquerque, New Mexico 87131, USA
[37]Northwestern University, Evanston, Illinois 60208, USA
[38]The Ohio State University, Columbus, Ohio 43210, USA
[39]Okayama University, Okayama 700-8530, Japan
[40]Osaka City University, Osaka 588, Japan
[41]University of Oxford, Oxford OX1 3RH, United Kingdom
[42]University of Padova, Istituto Nazionale di Fisica Nucleare, Sezione di Padova-Trento, I-35131 Padova, Italy
[43]LPNHE, Universite Pierre et Marie Curie/IN2P3-CNRS, UMR7585, Paris, F-75252 France
[44]University of Pennsylvania, Philadelphia, Pennsylvania 19104, USA
[45]Istituto Nazionale di Fisica Nucleare Pisa, Universities of Pisa, Siena and Scuola Normale Superiore, I-56127 Pisa, Italy
[46]University of Pittsburgh, Pittsburgh, Pennsylvania 15260, USA
[47]Purdue University, West Lafayette, Indiana 47907, USA
[48]University of Rochester, Rochester, New York 14627, USA
[49]The Rockefeller University, New York, New York 10021, USA
[50]Istituto Nazionale di Fisica Nucleare, Sezione di Roma 1, University of Rome "La Sapienza," I-00185 Roma, Italy
[51]Rutgers University, Piscataway, New Jersey 08855, USA
[52]Texas A&M University, College Station, Texas 77843, USA
[53]Istituto Nazionale di Fisica Nucleare, University of Trieste/ Udine, Italy
[54]University of Tsukuba, Tsukuba, Ibaraki 305, Japan
[55]Tufts University, Medford, Massachusetts 02155, USA
[56]Waseda University, Tokyo 169, Japan
[57]Wayne State University, Detroit, Michigan 48201, USA
[58]University of Wisconsin, Madison, Wisconsin 53706, USA
[59]Yale University, New Haven, Connecticut 06520, USA

(Received 23 November 2007; published 11 March 2008)

Inclusive jet cross sections in $Z/\gamma^*$ events, with $Z/\gamma^*$ decaying into an electron-positron pair, are measured as a function of jet transverse momentum and jet multiplicity in $p\overline{p}$ collisions at $\sqrt{s} = 1.96$ TeV with the upgraded Collider Detector at Fermilab in run II, based on an integrated luminosity of 1.7 fb$^{-1}$. The measurements cover the rapidity region $|y^{\text{jet}}| < 2.1$ and the transverse momentum range $p_T^{\text{jet}} > 30$ GeV$/c$. Next-to-leading order perturbative QCD predictions are in good agreement with the measured cross sections.

DOI: 10.1103/PhysRevLett.100.102001 PACS numbers: 13.85.−t, 12.38.Qk, 13.87.−a

The measurement of the inclusive production of collimated jets of hadrons in association with a $Z/\gamma^*$ boson in $p\overline{p}$ collisions provides a stringent test of perturbative quantum chromodynamics (pQCD) [1], and is sensitive to the presence of new particles decaying into $Z/\gamma^*$ + jets final states. At the leading order (LO) in pQCD, $Z/\gamma^*$ + jet events are driven by the processes $gq \rightarrow Z/\gamma^* + q$ and $q\overline{q} \rightarrow Z/\gamma^* + g$, while higher orders contributions, including additional parton radiation, produce mutiple jets in the final state. Next-to-leading order (NLO) pQCD predictions [2] for $Z/\gamma^*$ + jets production are only available for jet multiplicities $N_{\text{jet}}$ up to $N_{\text{jet}} = 2$. The understanding of $Z/\gamma^*$ + jets final states from data is therefore crucial since they also constitute important irreducible backgrounds in searches for new physics. Previous results [3] from run I at the Tevatron have been compared with LO plus parton shower Monte Carlo predictions affected by large scale uncertainties. This Letter reports new and more precise measurements of the inclusive jet cross sections in $Z/\gamma^*(\to e^+e^-)$ production using 1.7 $\text{fb}^{-1}$ of data collected by the CDF experiment in run II. The data are compared to NLO pQCD predictions including nonperturbative contributions.

The CDF II detector is described in detail elsewhere [4]. The detector has a charged particle tracking system immersed in a 1.4 T magnetic field aligned coaxially with the beam line that provides tracking coverage in the pseudorapidity [5] range $|\eta| \leq 2$. Segmented sampling calorimeters, arranged in a projective tower geometry, surround the tracking system and measure the energy of interacting particles for $|\eta| < 3.6$. The central electromagnetic and hadronic calorimeters cover the region $|\eta| < 1$, while the end-wall hadronic calorimeter provides forward coverage out to $|\eta| < 1.3$. Forward electromagnetic and hadronic calorimeters cover the regions $1.1 < |\eta| < 3.6$ and $1.3 < |\eta| < 3.6$, respectively. The calorimeters are instrumented with finely segmented detectors to measure the shower profile at a longitudinal depth close to the location of a typical electromagnetic shower maximum. Cherenkov counters in the region $3.7 < |\eta| < 4.7$ measure the number of inelastic $p\bar{p}$ collisions to compute the luminosity [6].

Samples of simulated inclusive $Z/\gamma^*(\to e^+e^-) + \text{jets}$ events are generated using the PYTHIA 6.216 [7] Monte Carlo generator. CTEQ5L [8] parton distribution functions (PDFs) are used for the proton and antiproton. The PYTHIA samples are created using a special tuned set of parameters, denoted as PYTHIA-TUNE A [9], that includes enhanced contributions from initial-state gluon radiation and secondary parton interactions between proton and antiproton beam remnants and provides an accurate description of the measured jet shapes and energy flows in $Z/\gamma^*(\to e^+e^-) + \text{jets}$ final states [10]. Monte Carlo samples for background processes are generated using PYTHIA-TUNE A. The samples are passed through a full CDF detector simulation (based on GEANT3 [11] where the GFLASH [12] package is used to simulate the energy deposition in the calorimeters) and reconstructed and analyzed with the same analysis chain as for the data.

Events are collected using a three-level trigger system [13]. At the first-level trigger, events are required to have a central electromagnetic calorimeter cluster ($|\eta| < 1$) with $E_T$ [5] above 8 GeV and an associated track with $p_T^{\text{track}}$ above 8 GeV$/c$. Similarly, at the second-level (third-level) trigger, a central electromagnetic cluster with $E_T > 16$ GeV ($E_T > 18$ GeV) and an associated track with $p_T^{\text{track}} > 8$ GeV$/c$ ($p_T^{\text{track}} > 9$ GeV$/c$) are required. The events are then required to have two electrons [14] with $E_T^e > 25$ GeV and a reconstructed invariant mass in the range $66 < M_{ee} < 116$ GeV$/c^2$ around the $Z$ boson mass. The electron candidates are reconstructed using criteria described in [15]. In this study, one electron is required to be central ($|\eta^e| < 1$) and fulfill tight selection cuts, while the second electron is required to pass a looser selection and to be either central (CC final-state configuration) or forward with $1.2 < |\eta^e| < 2.8$ (CF final-state configuration). The trigger efficiencies for CC and CF configurations are $99.96 \pm 0.01\%$ and $97.9 \pm 0.3\%$, respectively. The events are selected to have a reconstructed primary vertex with $z$ position within 60 cm around the nominal interaction point, and at least one jet with corrected transverse momentum $p_{T,\text{cor}}^{\text{jet}} > 30$ GeV$/c$ (see below), rapidity [5] in the range $|y_{\text{cal}}^{\text{jet}}| < 2.1$, and $\Delta R_{e-jet} > 0.7$, where $\Delta R_{e-jet}$ denotes the distance ($y-\phi$ space) between the jet and each of the two electrons in the final state. The final sample contains 6203, 650, 57, and 2 events with at least one, two, three, and four jets, respectively.

Jets are reconstructed in data and Monte Carlo simulated events using calorimeter towers with transverse momenta [16] above 0.1 GeV$/c$. The towers associated with the reconstructed electrons in the final state are excluded from the jet search. Jets are searched for using the midpoint algorithm [17] with cone radius $R = 0.7$ and a merging/splitting fraction of 0.75, starting from seed towers with transverse momenta above 1 GeV$/c$. The same algorithm is applied to the final state particles in the Monte Carlo generated events, excluding $Z/\gamma^*$ decay products, to define jets at the hadron level [18].

The rapidity and azimuthal angle of the jets, $y_{\text{cal}}^{\text{jet}}$ and $\phi_{\text{cal}}^{\text{jet}}$, are well reconstructed in the calorimeter with a resolution better than 0.05 units in both $y$ and $\phi$. The measured jet transverse momentum $p_{T,\text{cal}}^{\text{jet}}$ systematically underestimates that of the hadron-level jet. For $p_{T,\text{cal}}^{\text{jet}}$ values about 30 GeV$/c$, the jet transverse momentum is underestimated by about 30%. The systematic shift decreases with increasing $p_{T,\text{cal}}^{\text{jet}}$ down to about 11% for $p_{T,\text{cal}}^{\text{jet}} > 200$ GeV$/c$. This is mainly attributed to the presence of inactive material and the noncompensating nature of the calorimeter [19]. An average correction, as a function of $p_{T,\text{cal}}^{\text{jet}}$ and $y_{\text{cal}}^{\text{jet}}$, is applied to the measured $p_{T,\text{cal}}^{\text{jet}}$ to account for these effects [20]. The measured $p_{T,\text{cal}}^{\text{jet}}$ also includes contributions from multiple $p\bar{p}$ interactions per crossing at high instantaneous luminosity. Multiple interactions are identified via the presence of additional primary vertices reconstructed from charged particles. For each jet, $p_{T,\text{cal}}^{\text{jet}}$ is corrected for this effect by removing a certain amount of transverse momentum, $\delta_{p_T}^{\text{mi}} = 1.06 \pm 0.32$ GeV$/c$, for each additional primary vertex in the event, as determined from data [20].

The main backgrounds to the $Z/\gamma^*(\to e^+e^-) + \text{jets}$ sample arise from inclusive jets and $W + \text{jets}$ events, and are estimated from the data. First, an inclusive jet data sample is employed to estimate the probability $f_e^{\rm jet}$ for a jet to pass a given electron selection. The probabilities are parametrized as a function of $p_{T,\rm cal}^{\rm jet}$ and are typically around 0.001 (0.02) for tight (loose) central electrons and 0.005 for forward electrons. Second, a sample of events in data with exactly one reconstructed tight central electron is selected. For each jet in the event, the $E_T^e$ of a fake electron is determined, and the invariant mass of the tight-central electron and jet final state is then computed. Event-by-event, all electron-jet combinations that fulfill the $E_T^e$ cuts and with an invariant mass within $66 < M_{e-jet} < 116\ {\rm GeV}/c^2$ are considered in the background calculation, where each combination is weighted by the corresponding $f_{\rm e}^{\rm jet}$ value and divided by the number of accepted electron-jet combinations in the event. The total inclusive jets and $W$ + jets background is then computed in each measured distribution. Other background contributions from $t\bar{t}$, $Z/\gamma^*(\to e^+e^-) + \gamma$, $WW$, $WZ$, $ZZ$, and $Z/\gamma^*(\to \tau^+\tau^-)$ + jets final states are estimated using Monte Carlo samples. The total background in inclusive $Z/\gamma^*(\to e^+e^-)$ + jets production is about 12% for $N_{\rm jet} \geq 1$, and increases up to about 17% for $N_{\rm jet} \geq 3$.

Raw inclusive jet differential cross sections as a function of $p_{T,\rm cor}^{\rm jet}$ are defined as $d\sigma/dp_{T,\rm cor}^{\rm jet} = \frac{1}{\mathcal{L}} \times (N_{\rm jet}^{\rm cor}/\Delta p_{T,\rm cor}^{\rm jet})$, where $N_{\rm jet}^{\rm cor}$ denotes the total number of jets in a given $p_{T,\rm cor}^{\rm jet}$ bin, $p_{T,\rm cor}^{\rm jet}$ is the size of the bin, and $\mathcal{L}$ is the luminosity. $N_{\rm jet}^{\rm cor}$ is corrected bin-by-bin for background contributions and trigger inefficiencies. The measured cross sections are then corrected for acceptance and smearing effects back to the hadron level using PYTHIA-TUNE A Monte Carlo event samples, and a bin-by-bin unfolding procedure that also accounts for the efficiency of the $Z/\gamma^*(\to e^+e^-)$ selection criteria. The final results refer to hadron-level jets with $p_T^{\rm jet} > 30\ {\rm GeV}/c$ and $|y^{\rm jet}| < 2.1$, in a limited and well-defined kinematic range for the $Z/\gamma^*$ decay products: $E_T^e > 25$ GeV, $|\eta^{e1}| < 1.0$, $|\eta^{e2}| < 1.0$ or $1.2 < |\eta^{e2}| < 2.8$, $66 < M_{ee} < 116\ {\rm GeV}/c^2$, and $\Delta R_{e-jet} > 0.7$. In order to avoid any bias on the correction factors due to the particular PDF set used, which translates into slightly different simulated $p_{T,\rm cal}^{\rm jet}$ distributions, the PYTHIA-TUNE A Monte Carlo event sample is reweighted until it accurately follows the measured $p_{T,\rm cal}^{\rm jet}$ spectra. The unfolding factors $U(p_{T,\rm cor}^{\rm jet}) = \frac{d\sigma}{dp_T^{\rm jet}} / \frac{d\sigma}{dp_{T,\rm cor}^{\rm jet}}$ are computed separately for the different measurements and vary between 2.0 at low $p_T^{\rm jet}$ and 2.3 at high $p_T^{\rm jet}$.

A detailed study of the systematic uncertainties was carried out [10]. A $\pm 1.5\%$ uncertainty on the trigger efficiency translates into $\pm 1.5\%$ and $\pm 0.06\%$ uncertainties on the cross sections for CF and CC configurations, respectively. The uncertainty on the $p_T^{\rm jet}$ dependence of the electron identification efficiency introduces a $\pm 5\%$ uncertainty on both CC and CF results. The measured jet energies are varied by $\pm 2\%$ at low $p_{T,\rm cal}^{\rm jet}$ to $\pm 2.7\%$ at high $p_{T,\rm cal}^{\rm jet}$ to account for the uncertainties on the absolute energy scale in the calorimeter [20]; this introduces uncertainties on the final measurements which vary between $\pm 5\%$ at low $p_T^{\rm jet}$ and $\pm 12\%$ at high $p_T^{\rm jet}$. The $y^{\rm jet}$ dependence of the average correction applied to $p_{T,\rm cal}^{\rm jet}$ introduces a $\pm 2\%$ uncertainty on the measured cross sections, approximately independent of $p_T^{\rm jet}$. The uncertainty on $\delta_{p_T}^{\rm mi}$ has a negligible effect on the measured cross sections. The uncertainty on the $p_{T,\rm cal}^{\rm jet}$ dependence of $f_e^{\rm jet}$ introduces a $\pm 15\%$ uncertainty on the inclusive jets and $W$ + jets background estimation, that translates into a less than 2% uncertainty on the measured cross sections. A conservative $\pm 30\%$ uncertainty on the normalization of the rest of the background contributions, as extracted from Monte Carlo samples, introduces a less than 1% effect on the final results. If the unfolding procedure is carried out using unweighted PYTHIA-TUNE A, the effect on the measured cross sections is less than 1%. Positive and negative deviations with respect to the nominal cross section values are added separately in quadrature to define the total systematic uncertainty. The final results are obtained from the combination of CC and CF measurements. Finally, a 5.8% uncertainty on the total luminosity [15] is included in the measured cross sections.

Figure 1(a) shows the measured inclusive jet differential cross sections as a function of $p_T^{\rm jet}$ in $Z/\gamma^*(\to e^+e^-)$ + jets production, with $N_{\rm jet} \geq 1$ and $N_{\rm jet} \geq 2$, compared to NLO pQCD predictions. The data are reported in Table I. The cross sections decrease by more than 3 orders of magnitude as $p_T^{\rm jet}$ increases from 30 GeV/$c$ up to about 300 GeV/$c$. The NLO pQCD predictions are computed using the MCFM program [2] with CTEQ6.1M PDFs [21], with the renormalization and factorization scales set to $\mu^2 = M_Z^2 + p_T^2(Z)$, and using a midpoint algorithm with $R = 0.7$ and $R_{\rm sep} = 1.3$ [22] to reconstruct jets at the parton level. Values for $R_{\rm sep}$ between 1.0 and 2.0 change the theoretical prediction by less than 2%. A variation of $\mu$ by a factor of two (half) reduces (increases) the theoretical predictions by 10% to 15%. The uncertainties on the NLO pQCD predictions due to the PDFs were computed using the Hessian method [23]. They vary from $\pm 4\%$ at low $p_T^{\rm jet}$ to $\pm 10\%$ at high $p_T^{\rm jet}$.

The theoretical predictions include parton-to-hadron correction factors $C_{\rm had}(N_{\rm jet}, p_T^{\rm jet})$ that approximately account for nonperturbative contributions from the underlying event and fragmentation into hadrons (see Table I). In each measurement, $C_{\rm had}$ is estimated using the PYTHIA-TUNE A Monte Carlo samples, as the ratio between the nominal $p_T^{\rm jet}$ distribution and the one obtained by turning off both the interactions between proton and antiproton remnants and the string fragmentation in the Monte Carlo

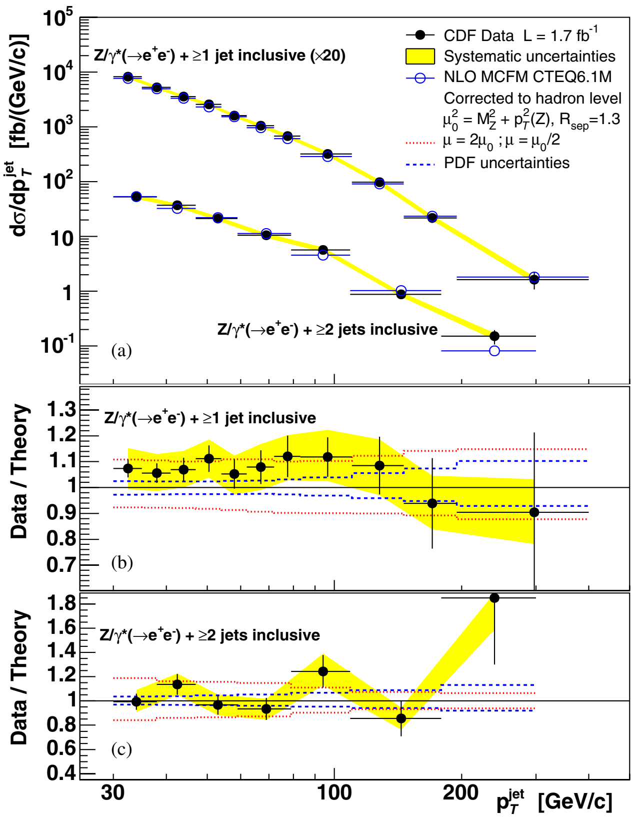


FIG. 1 (color online). (a) Measured inclusive jet differential cross section as a function of $p_T^{\rm jet}$ (black dots) in $Z/\gamma^*(\to e^+e^-) + $ jets with $N_{\rm jet} \geq 1, 2$ compared to NLO pQCD predictions (open circles). For clarity, the measurement for $N_{\rm jet} \geq 1$ is scaled up ($\times 20$). The shaded bands show the total systematic uncertainty, except for the 5.8% luminosity uncertainty. (b) and (c) Data/theory ratio as a function of $p_T^{\rm jet}$ for $N_{\rm jet} \geq 1$ and $N_{\rm jet} \geq 2$, respectively. The dashed and dotted lines indicate the PDF uncertainty and the variation with $\mu$ of the NLO pQCD predictions, respectively.

samples. The correction decreases as $p_T^{\rm jet}$ increases from about 1.2 (1.26) at $p_T^{\rm jet}$ of 30 GeV/$c$ to 1.02 (1.01) for $p_T^{\rm jet} > 200$ GeV/$c$ for $N_{\rm jet} \geq 1$ ($N_{\rm jet} \geq 2$), and is dominated by the underlying event contribution. In order to estimate the uncertainty on $C_{\rm had}$, PYTHIA samples are generated with a different set of parameters, denoted as TUNE DW [24], that governs the underlying event activity and also describes the $Z/\gamma^*(\to e^+e^-) + $ jets final states. The uncertainty on $C_{\rm had}$ is about 10% (17%) at low $p_T^{\rm jet}$ and goes down to 1% at high $p_T^{\rm jet}$ for $N_{\rm jet} \geq 1$ ($N_{\rm jet} \geq 2$). The ratios between data and theory as a function of $p_T^{\rm jet}$ are shown in Figs. 1(b) and 1(c). Good agreement is observed between the measured cross sections and the nominal theoretical predictions. A $\chi^2$ test, where the sources of systematic uncertainty on the data are considered independent but fully correlated across $p_T^{\rm jet}$ bins, and the uncertainty on

TABLE I. Measured inclusive jet differential cross section in $Z/\gamma^*(\to e^+e^-)$+jets production as a function of $p_T^{\rm jet}$ with $N_{\rm jet} \geq 1$ and $N_{\rm jet} \geq 2$. The systematic uncertainties are fully correlated across $p_T^{\rm jet}$ bins. The parton-to-hadron correction factors $C_{\rm had}(p_T^{\rm jet}, N_{\rm jet})$ are applied to the pQCD predictions.

| $p_T^{\rm jet}$ [GeV/$c$] | $\frac{d\sigma}{dp_T^{\rm jet}}$ ± (stat) ± (syst) ± (lum) [fb/(GeV/$c$)] | $C_{\rm had}$ ± (stat) ± (syst) parton → hadron |
|---|---|---|
| | $Z/\gamma^*(\to e^+e^-)$ + jets | ($N_{\rm jet} \geq 1$) |
| 30–35 | $413.3 \pm 13.3^{+30.4}_{-31.3} \pm 24.0$ | $1.209 \pm 0.010 \pm 0.134$ |
| 35–41 | $263.3 \pm 9.4^{+18.3}_{-17.4} \pm 15.3$ | $1.146 \pm 0.010 \pm 0.096$ |
| 41–47 | $178.3 \pm 7.5^{+12.0}_{-11.6} \pm 10.3$ | $1.114 \pm 0.011 \pm 0.077$ |
| 47–54 | $128.5 \pm 5.9^{+8.7}_{-8.4} \pm 7.5$ | $1.097 \pm 0.012 \pm 0.066$ |
| 54–62 | $80.5 \pm 4.3^{+5.5}_{-6.0} \pm 4.7$ | $1.086 \pm 0.013 \pm 0.059$ |
| 62–72 | $52.5 \pm 3.2^{+4.4}_{-4.3} \pm 3.0$ | $1.078 \pm 0.013 \pm 0.053$ |
| 72–83 | $34.2 \pm 2.4^{+2.5}_{-2.8} \pm 2.0$ | $1.072 \pm 0.015 \pm 0.049$ |
| 83–110 | $16.0 \pm 1.1^{+1.5}_{-1.3} \pm 0.9$ | $1.063 \pm 0.012 \pm 0.043$ |
| 110–146 | $4.9 \pm 0.5^{+0.5}_{-0.5} \pm 0.3$ | $1.051 \pm 0.012 \pm 0.035$ |
| 146–195 | $1.1 \pm 0.2^{+0.1}_{-0.1} \pm 0.06$ | $1.040 \pm 0.008 \pm 0.027$ |
| 195–400 | $0.08 \pm 0.03^{+0.01}_{-0.01} \pm 0.005$ | $1.021 \pm 0.005 \pm 0.013$ |
| | $Z/\gamma^*(\to e^+e^-)$ + jets | ($N_{\rm jet} \geq 2$) |
| 30–38 | $52.9 \pm 3.5^{+5.3}_{-4.6} \pm 3.1$ | $1.262 \pm 0.022 \pm 0.217$ |
| 38–47 | $37.0 \pm 2.8^{+2.9}_{-2.8} \pm 2.1$ | $1.207 \pm 0.024 \pm 0.169$ |
| 47–59 | $21.2 \pm 1.8^{+1.9}_{-1.9} \pm 1.2$ | $1.164 \pm 0.025 \pm 0.130$ |
| 59–79 | $10.5 \pm 1.0^{+0.9}_{-1.0} \pm 0.6$ | $1.123 \pm 0.024 \pm 0.093$ |
| 79–109 | $5.7 \pm 0.6^{+0.7}_{-0.5} \pm 0.3$ | $1.087 \pm 0.026 \pm 0.062$ |
| 109–179 | $0.88 \pm 0.15^{+0.09}_{-0.10} \pm 0.05$ | $1.052 \pm 0.020 \pm 0.030$ |
| 179–300 | $0.15 \pm 0.04^{+0.02}_{-0.02} \pm 0.009$ | $1.026 \pm 0.010 \pm 0.008$ |

$C_{\rm had}$ is also included, gives a $\chi^2$ probability of 99% (22%) for $N_{\rm jet} \geq 1$ ($N_{\rm jet} \geq 2$).

Figure 2 shows the cross sections $\sigma_{N_{\rm jet}}$ for $Z/\gamma^*(\to e^+e^-) + $ jets events up to $N_{\rm jet} \geq 3$. The measured event cross sections are $\sigma_1 = 7003 \pm 146({\rm stat})^{+483}_{-470}({\rm syst}) \pm 406({\rm lum})$ fb, $\sigma_2 = 695 \pm 37({\rm stat})^{+59}_{-60}({\rm syst}) \pm 40({\rm lum})$ fb, and $\sigma_3 = 60 \pm 11({\rm stat})^{+8}_{-8}({\rm syst}) \pm 3.5({\rm lum})$ fb, for $N_{\rm jet} \geq 1$, $N_{\rm jet} \geq 2$, and $N_{\rm jet} \geq 3$, respectively. The data are compared to LO and NLO pQCD predictions. The parton-to-hadron nonperturbative corrections vary between 1.1 and 1.4 as $N_{\rm jet}$ increases. The LO pQCD predictions underestimate the measured cross sections by a factor about 1.4 approximately independent of $N_{\rm jet}$. For $N_{\rm jet} \geq 1$ and $N_{\rm jet} \geq 2$, this corresponds to $\chi^2$ probabilities of 0.07% and 2.7%, respectively. Good agreement is observed between data and NLO pQCD predictions, with $\chi^2$ probabilities better than 83%.

In summary, we report new results on inclusive jet production in $Z/\gamma^*(\to e^+e^-)$ events in $p\bar{p}$ collisions at

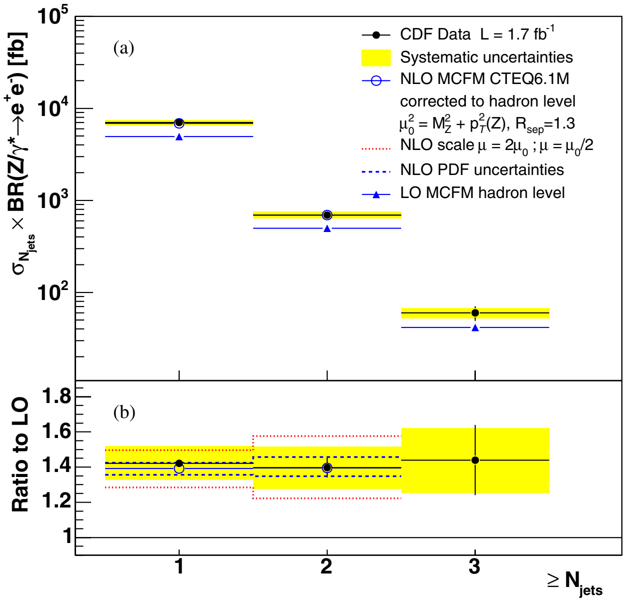


FIG. 2 (color online). (a) Measured cross section for inclusive jet production in $Z/\gamma^*(\to e^+e^-)$ events as a function of $N_{\rm jet}$ compared to LO and NLO pQCD predictions. The shaded bands show the total systematic uncertainty, except for the 5.8% luminosity uncertainty. (b) Ratio of data and NLO to LO pQCD predictions versus $N_{\rm jet}$. The dashed and dotted lines indicate the PDF uncertainty and the variation with $\mu$ of the NLO pQCD predictions, respectively.

$\sqrt{s} = 1.96$ TeV for jets with $p_T^{\rm jet} > 30$ GeV$/c$ and $|y^{\rm jet}| < 2.1$, based on 1.7 fb$^{-1}$ of CDF run II data. The measured cross sections are well described by NLO pQCD predictions including nonperturbative corrections.

We thank the Fermilab staff and the technical staffs of the participating institutions for their vital contributions. This work was supported by the U.S. Department of Energy and National Science Foundation; the Italian Istituto Nazionale di Fisica Nucleare; the Ministry of Education, Culture, Sports, Science and Technology of Japan; the Natural Sciences and Engineering Research Council of Canada; the National Science Council of the Republic of China; the Swiss National Science Foundation; the A.P. Sloan Foundation; the Bundesministerium für Bildung und Forschung, Germany; the Korean Science and Engineering Foundation and the Korean Research Foundation; the Science and Technology Facilities Council and the Royal Society, UK; the Institut National de Physique Nucleaire et Physique des Particules/CNRS; the Russian Foundation for Basic Research; the Comisión Interministerial de Ciencia y Tecnología, Spain; the European Community's Human Potential Programme; the Slovak R&D Agency; and the Academy of Finland.

[a]IFIC(CSIC-Universitat de Valencia), 46071 Valencia, Spain.
[b]Visitor from Universidad Iberoamericana, Mexico D.F., Mexico.
[c]Visitor from Queen Mary, University of London, London, E1 4NS, England.
[d]Visitor from University de Oviedo, E-33007 Oviedo, Spain.
[e]Visitor from University Libre de Bruxelles, B-1050 Brussels, Belgium.
[f]Visitor from University of Athens, 15784 Athens, Greece.
[g]Visitor from University of Bristol, Bristol BS8 1TL, United Kingdom.
[h]Visitor from TX Tech University, Lubbock, TX 79409, USA.
[i]Visitor from University of Edinburgh, Edinburgh EH9 3JZ, United Kingdom.
[j]Visitor from University College Dublin, Dublin 4, Ireland.
[k]Visitor from University of Heidelberg, D-69120 Heidelberg, Germany.
[l]Visitor from University of CA Santa Cruz, Santa Cruz, CA 95064, USA.
[m]Visitor from University of Cyprus, Nicosia CY-1678, Cyprus.
[n]Visitor from Nagasaki Institute of Applied Science, Nagasaki, Japan.
[o]Visitor from University of CA Irvine, Irvine, CA 92697, USA.
[p]Visitor from Cornell University, Ithaca, NY 14853, USA.
[q]Visitor from University of Manchester, Manchester M13 9PL, England.
[r]Visitor from Chinese Academy of Sciences, Beijing 100864, China.

[1] D. J. Gross and F. Wilczek, Phys. Rev. D **8**, 3633 (1973).
[2] J. Campbell and R. K. Ellis, Phys. Rev. D **65**, 113007 (2002).
[3] T. Affolder *et al.* (CDF Collaboration), Phys. Rev. D **63**, 072003 (2001).F. Abe *et al.* (CDF Collaboration), Phys. Rev. Lett. **77**, 448 (1996).
[4] D. Acosta *et al.* (CDF Collaboration), Phys. Rev. D **71**, 032001 (2005).
[5] We use a cylindrical coordinate system about the beam axis with polar angle $\theta$ and azimuthal angle $\phi$. We define $E_T = E\sin\theta$, $p_T = p\sin\theta$, pseudorapidity $\eta = -\ln[\tan(\frac{\theta}{2})]$, and rapidity $y = \frac{1}{2}\ln(\frac{E+p_z}{E-p_z})$.
[6] D. Acosta *et al.*, Nucl. Instrum. Methods Phys. Res., Sect. A **494**, 57 (2002).
[7] T. Sjöstrand *et al.*, Comput. Phys. Commun. **135**, 238 (2001).
[8] H. L. Lai *et al.*, Eur. Phys. J. C **12**, 375 (2000).
[9] T. Affolder *et al.* (CDF Collaboration), Phys. Rev. D **65**, 092002 (2002).
[10] O. Saltó, Ph.D. thesis, U.A.B., Barcelona, 2008.
[11] R. Brun *et al.*, Technical Report No. CERN-DD/EE/84-1, 1987.
[12] G. Grindhammer, M. Rudowicz, and S. Peters, Nucl. Instrum. Methods Phys. Res., Sect. A **290**, 469 (1990).
[13] B. L. Winer, Int. J. Mod. Phys. A **16S1C**, 1169 (2001).
[14] Charge conjugation is implied throughout the Letter.
[15] A. Abulencia *et al.* (CDF Collaboration), J. Phys. G **34**, 2457 (2007).

[16] The momentum is computed using the energy and the position with respect to the primary interaction vertex.
[17] A. Abulencia *et al.* (CDF Collaboration), Phys. Rev. D **74**, 071103(R) (2006).
[18] The hadron level in the Monte Carlo generators is defined using all final-state particles with lifetimes above $10^{-11}$ s.
[19] S. R. Hahn *et al.*, Nucl. Instrum. Methods Phys. Res., Sect. A **267**, 351 (1988).
[20] A. Bhatti *et al.*, Nucl. Instrum. Methods Phys. Res., Sect. A **566**, 375 (2006).
[21] J. Pumplin *et al.*, J. High Energy Phys. 07 (2002) 012.
[22] S. D. Ellis and D. E. Soper, Phys. Rev. D **48**, 3160 (1993).
[23] J. Pumplin *et al.*, Phys. Rev. D **65**, 014013 (2001).
[24] R. Field, FERMILAB-CONF-06-408-E, FNAL, 2005.